Journal of Fluorescence (2020) 30:131–142
https://doi.org/10.1007/s10895-019-02478-x

ORIGINAL ARTICLE

Binding Properties of DNA and Antimicrobial Peptide Chensinin-1b Containing Lipophilic Alkyl Tails

Weibing Dong [1,2] · Xueyue Luo [1] · Yue Sun [1,2] · Yue Li [1] · Cui Wang [1,3] · Yue Guan [1] · Dejing Shang [1,2]

Received: 22 August 2019 / Accepted: 26 December 2019 / Published online: 10 January 2020

Abstract

Multidrug-resistant bacteria present an important threat to human health. In this study, due to the weak antimicrobial activity of chensinin-1b against multidrug-resistant (MDR) bacteria, three lipo-chensinin-1b peptides, including OA-C1b, LA-C1b and PA-C1b, were designed and their activities against MDR bacteria were examined. Both the OA-C1b and LA-C1b peptides exhibited potent antimicrobial activity against selected multidrug-resistant bacterial strains. In addition to the direct disruption of bacterial membranes by antimicrobial peptides, it has also been proposed that DNA is a superior intracellular target for antimicrobial peptides. ctDNA was used as a model to investigate the binding properties of DNA and lipo-chensinin-1b peptides using a variety of biophysical methods. The kinetics results of both UV-Vis and CD spectroscopy suggested that the interaction between lipo-chensinin-1b peptides and ctDNA was concentration-dependent and resulted in an increase in polynucleotide helicity. Viscosity measurements, Trp fluorescence and iodide quenching experiments indicated that nonclassical groove binding and electrostatic binding interaction modes were utilized when the peptides interacted with the ctDNA. In addition, the formation of peptide-ctDNA complexes was monitored using dynamic light scattering experiments, during which the peptide exhibited the ability to neutralize the negative charges on the surface of the ctDNA. These results promote the possibility of designing peptide-based antibiotics targeted to DNA.

Keywords Antimicrobial peptide · DNA · Binding interaction · Aliphatic acid · Multidrug-resistant bacteria

Introduction

The over-prescribing of conventional antibiotics has resulted in the emergence of multidrug-resistant pathogens, which pose a serious public-health problem. Antimicrobial peptides (AMPs) from natural sources have attracted much attention from researchers due to their potential to function as novel antibiotics, which is the result of their unique mechanisms of action during interaction with the bacteria [1–4]. Generally, AMPs kill bacterial cells mainly via two different hypothetical mechanisms: barrel stave model in which the amphipathic peptide form bundles and their hydrophobic surfaces interact with the lipid core of the membrane and point inward to produce a pore, and carpet models in which the amphipathic peptides initially bind onto the surface of the target membrane and cover the membrane like a carpet-like manner [5–8]. Using the mechanisms described above, antimicrobial peptides can initially bind to the outer membranes of the bacterial cell via electrostatic interactions, destabilize the integrity of the cell membrane, and ultimately lyse the bacterial cell [9, 10]. In addition to interacting with cells via these three mechanisms, some antimicrobial peptides can also penetrate the bacterial cell membrane, where they bind to intracellular DNA and RNA, that which will further inhibit cellular functioning and induce cell death. For example, the antimicrobial peptide buforin II can kill bacteria without disrupting the cells, but rather by penetrating the cell membrane and interacting

Weibing Dong, Xueyue Luo and Yue Sun contributed equally to this work.

Electronic supplementary material The online version of this article (https://doi.org/10.1007/s10895-019-02478-x) contains supplementary material, which is available to authorized users.

✉ Dejing Shang
djshang@lnnu.edu.cn

[1] School of Life Science, Liaoning Normal University, Dalian 116081, China

[2] Liaoning Provincial Key Laboratory of Biotechnology and Drug Discovery, Liaoning Normal University, Dalian 116081, China

[3] Department of Neurology, Dalian Municipal Central Hospital, Dalian 116033, China

with intracellular DNA or RNA with strong affinity [11]. Other examples are the antimicrobial peptide PR-39 and tachyplesin I, which can also bind tightly to DNA and RNA and thereby inhibit macromolecular synthesis in the cell [12]. Generally, DNA plays an important role in vital biological processes, including gene expression, mutagenesis, and gene transcription, and represents an ideal intracellular target for various drugs [13, 14]. Therefore, the mechanisms utilized by pharmaceutical agents to bind to DNA have been widely studied during the past few decades. This has led to the proposal of the existence of three major non-covalent interaction modes that include intercalative binding between stacked base pairs (causing DNA structural distortion), groove binding, and weak binding resulting from electrostatic interactions [15, 16]. During a recent study in which calf thymus DNA (ctDNA) was used as a representative DNA molecule, the binding mode utilized between ctDNA and small molecules was characterized using various biophysical methods to generate an interaction model that could yield valuable information for the development of targeted therapeutics [17–19].

During our previous research, a novel antimicrobial peptide, chensinin-1b, was designed according to the sequence of the natural peptide chensinin-1, which is isolated from skin secretions of the Chinese brown frog *Rana chensinensis* [10]. Compared with chensinin-1, the designed chensinin-1b peptide analog exhibited potent broad-spectrum antimicrobial activity due to its enhanced hydrophobicity and amphipathicity. Investigation of the antimicrobial mechanism utilized by chensinin-1b suggested that the peptide lysed the bacterial cell membrane through the carpet mechanism. However, chensinin-1b exhibited no activity against the specific cancer cell lines and only slight antimicrobial activity against the selected multidrug-resistant bacteria isolated from clinical specimens. To improve anticancer activity, three aliphatic analogs were designed and lipid acids were conjugated to the ^{17}Lys-residue in the sequence [20]. The resulting lipopeptides OA-C1b, LA-C1b and PA-C1b, exhibited much stronger activity to kill the selected bacteria than chensinin-1b. In addition, the lipo-chensinin-1b peptides were able to kill the specific cancer cell lines, and were able to inhibit LPS-induced cytokine release from U937 cells.

In this study, multidrug-resistant bacteria were isolated from patients and the capability of lipo-chensinin-1b peptides to kill these multidrug-resistant bacteria was examined. The binding characteristics between lipo-chensinin-1b peptides and calf thymus DNA were determined using various biophysical methods, including UV-Vis absorption, circular dichroism (CD) and fluorescence spectroscopy. In addition, the peptide concentration dependent UV-vis and CD spectra were monitored to detect ctDNA-lipochensinin-1b complex formation. This study provides insights into the specific molecular mechanisms utilized by antimicrobial peptides to bind to DNA.

Materials and Methods

Peptide

The synthesis of peptides was performed using standard Fmoc solid-phase peptide synthesis protocols (Karebay Biochem Ltd., Ningbo, China) according to the published procedures [20]. The aliphatic acids were attached to the amine group of the 17th lysine residue within the N-terminus ofchensinin-1b sequence, and the structures of each peptide were shown in Table S1. The crude peptides were obtained as $CH_3(CH_2)_6CO$-SKVWRHWRRFWHRAHRKL (OA-C1b), $CH_3(CH_2)_{10}CO$-SKVWRHWRRFWHRAHRKL (LA-C1b) and $CH_3(CH_2)_{14}CO$- SKVWRHWRRFWHRAHRKL (PA-C1b) with about 12.4%, 14.9% and 6% yields, respectively, and further purified using RP-HPLC and the purity used for the experiments was above 95%. The molecular weights were determined using ESI-MS.

Multidrug-Resistant Bacterial Strains

The multidrug-resistant strains that were used included *P. aeruginosa* 0108 (MRPA0108), *P. fluorescens* 0322 (MRPF0322), *E. cloacae* 0320 (MREC0320), *K. pneumonia*1112 (MRKP1112), *A.baumannii* 0227(MRAB0227), *E. aerogenes* 0320 (MREA0320), *S. aureus* 0910 (MRSA0910), *E. faecium* 0321 (MREF0321), and *E. coli* 0203 (MREC0203). These selected strains were clinically isolated from patients admitted to the First Affiliated Hospital of Dalian Medical University. The results of antibiotic susceptibility assays indicated that these bacterial strains showed resistance to ciprofloxacin, cefepime, amoxicillin, ampicillin, streptomycin, gentamicin, kanamycin and tetracycline.

Antibacterial Activity Assays

Assays of the ability of lipo-chensinin-1b to kill the selected multidrug-resistant bacterial strains were conducted according to the standard micro-dilution method [21]. The assigned peptides at an initial concentration of 200 μM were dissolved in PBS buffer and then serially diluted two-fold until a final concentration of 1.56 μM was obtained. 50 μL of peptide solution as aliquots was added to each well of a 96-well microtiter plate, to which an equal volume of log-phase bacterial inoculums (2×10^6 CFU/mL) was added. The final mixtures were incubated for 24 h at 37 °C. For each sample, the OD_{600} was detected on a microtiter plate reader. The minimal inhibitory concentration (MIC) was defined as the minimal concentration of the peptide in which bacterial growth was completely inhibited.

Scanning Electron Microscopy (SEM)

Multidrug-resistant *S. epidermidis* and *E. coli* cells were selected and incubated with the representative peptide OA-C1b at 1xMIC according to the published procedures [10]. The bacteria were collected and washed with PBS buffer. The pellets were fixed in cacodylate buffer (0.1 M, 2.5% glutaraldehyde) (Solarbio, Beijing, China). The bacteria cells were stained with osmium tetroxide (1%, Sigma-Aldrich, Shanghai, China) in buffer solution for 2 h and then dehydrated using ethanol. The samples were observed using a Hitachi SU8010 scanning electron microscope after lyophilization and coating processes were conducted.

Circular Dichroism (CD) Spectroscopy

The conformational changes in the ctDNA were detected via analysis of CD spectra upon interaction with the peptides; CD spectra derived from ctDNA with or without the existance of the chensinin-1b peptide and its analogs at various concentrations were obtained at room temperature using spectropolarimeter (Bio-Logic MOS-500, France) equipped with a 1-mm path length quartz cell and a defined wavelength rang of 220–360 nm. The ctDNA sample were dissolved in 10 mM sodium phosphate buffer (pH 7.0), at a 50 μM fixed concentration, while the peptide was added at actDNA: peptide ratio ranging from 1 to 5. The CD spectra produced by the buffer solution were recorded as the baseline. The ctDNA sample was added to the cuvette to record the spectra of the ctDNA. Peptides were added to the DNA sample solution at specific molar ratios, and the final solution were mixed well. The CD spectra were measured after 5 min of incubation for each peptide concentration.

UV-Spectroscopy

The absorption spectra of fixed concentration of ctDNA were recorded using a Bruker UV spectrophotometer. The ctDNA was incubated with peptides at various concentrations for 10 min; the molar ratio of ctDNA to peptide ranged from 0.5 to 8. The UV spectra for each peptide concentration were recorded and PBS buffer was used as a blank.

The Fluorescence Spectra of Trp Residues and Quenching

The fluorescence emission spectra derived from the intrinsic Trp residues within the peptide sequences were measured using a spectrofluorometer (Varioskan Flash, Thermo Scientific, Beijing, China) according to the published protocol [10]. The measurements of Trp-derived spectra for the peptides titrated in the presence of ctDNA were performed according to a previously reported method [22]. Aliquots of ctDNA were added to a 10 μM peptides solution in 5 mM TES buffer solution (pH 7.4) and incubated at 25 °C for 10 min. The excitation wavelength was set at 280 nm for the Trp residues, and the emission spectra between 300 and 400 nm were collected using 5-nm band passes. Fluorescence quenching experiments were performed that investigated the titration of peptides in the absence and/or presence of ctDNA, during which KI was used as a water-soluble quencher. The concentration of KI was varied from 20 to 140 mM in the wells, and the molar ratio of ctDNA:peptide ranged from 100:1 to 0:1. The excitation of Trp residues was performed at 295 nm and the emission was examined at 350 nm in order to reduce the absorbance effect by KI. The effects of KI on the fluorescence of each peptide were quantified according to the published methods [10]. The quenching data were analysed with the Sterne Volmer equation: $F_0/F = 1+ K_{sv}[Q]$, where F_0 and F are the fluorescence intensities at 350 nm in the absence and presence of a quencher at a concentration [Q], respectively. K_{sv} is the Sterne Volmer quenching constant.

Agarose Gel Electrophoresis

The ability of the peptides to bind to ctDNA was characterized using a previously described method [23]. The loading mixture contained 0.15 mM ctDNA (fixed concentration) and the varying concentrations of the peptides such that the molar ratio varied from 4:1 to 1:1 in each well. The final ctDNA-peptide solution was incubated for 30 min and mixed with 3 μL of ethidium bromide dye, and then the samples were loaded into the wells of the gel. The experiments were conducted at 80 V for 20 min using a TE buffer system. The bands were detected using a UV-transilluminator (Baygene, Beijing, China). The ability of the peptides to bind to ctDNA was using mobility and relative quantitative analysis, which was based on changes in the fluorescence intensity of the bands.

Viscosity Measurements

Viscometric titrations were conducted using an Ubbeholde viscometer at 25 °C and the data were analyzed according to a previously published procedure [19]. The specific *r* value (r = [peptide]/[ctDNA]) used to evaluate the viscosity was obtained from experiments during which an appropriate amount of the assigned peptide was added to the viscometer while ctDNA was added at a fixed concentration. The flow time was recorded, and the viscosity value (η) was calculated using the equation $\eta = (t\text{-}t_0)/t_0$, where the flow time for ctDNA-peptide solution was defined as t and that for the corrected blank ctDNA solution was defined as t_0. The measurements were performed in triplicate, and the viscosity of the complexes were determined as the mean of the three values. The data were plotted using $(\eta/\eta_0)^{1/3}$ to define the y-axis and the

[peptide]/[ctDNA] molar ratio to define the x-axis; η and η_0 represent the viscosity of the ctDNA with and without the presence of the peptides, respectively.

Dynamic Light Scattering and Zeta Potential Experiments

The size changes in the ctDNA with and without the peptides were monitored using dynamic light scattering experiments. The mixtures of 1 μM ctDNA either in the absence of peptide or in the presence of 2 μM peptide were initially filtered through a 0.45-μm filter and incubated for 60 min. The data were processed using the CONTIN method afforded by the software supplied by the instrument. The measurement of the peptide alone was used as a blank.

The zeta potential of the ctDNA with and without the specified peptides at concentrations that varied from 0 to 0.5 mM was determined using similar method as published [24]. In order to achieve a high count rate, the ctDNA concentration was set at 0.1 mM. The zeta-potential was determined using the Helmholtz-Smoluchowski equation: $u = \frac{\varepsilon}{\eta}\zeta$, where u is the electrophoretic mobility, $\varepsilon = \varepsilon_r^{es}\varepsilon_0$, in which ε_r^{es} and ε_0 are the relative dielectic constant of electrolyte solution and the dielectic constand of vacuum, respectively, and η is the viscosity of the solution [25], which is based on the mobility of the aggregates in a driving electric field of 19.2 Vcm^{-1}.

Results

Antibacterial Activity of Lipo-Chensinin-1b Peptides

The MICs of the lipo-chensinin-1b peptides against the specified MDR bacterial strains are presented in Table 1. OA-C1b showed potent antibacterial activity against all multidrug-resistant bacteria, and the MIC values obtained for specific bacterial strains were ranged from 3.12 to 50 μM. LA-C1b exhibited much lower activity against bacteria than OA-C1b, with the exception of *S. epidermidis* (MRSE1208; MIC at 12.5 μM). PA-C1b exhibited almost no antimicrobial activity against the selected bacterial strains (all MIC values were ≥ 100 μM).

Morphological Changes in OA-C1b-Treated *E. coli* and E. Epidermidis Cells

The morphological changes in selected bacterial strains incubated with the OA-C1b were examined using SEM as shown in Fig. 1. In the absence of peptide, both *E. coli* and *E. epidermidis* exhibited a normal, smooth surface. When the bacterial cells were treated with peptide at a concentration of 1xMIC, the partial disruption of cell surfaces in both bacterial strains was detected, and the protoplasm released by the bacteria exhibited viscidity.

Table 1 MIC of the peptides against the selected multidrug-resistant bacteria

Microorganism	MIC(μM)[a]			
	OA-C1b	LA-C1b	PA-C1b	Chensinin-1b
G^-				
E.coli	6.25	25	>100	1.56
P.aeruginosa	50	100	>100	25
A. baumannii	12.5	50	>100	25
E. aerogenes	25	100	>100	>50
E. cloacae	25	100	100	>50
P. fluorescens	12.5	50	>100	>50
K. pneumonia	25	50	100	50
G^+				
S.aureus	6.25	25	>100	3.13
S. epidermidis	3.13	12.5	>100	12.5
E.faecium	3.13	100	100	6.25

[a] Minimum inhibitory concentration (MIC) was determined as the lowest concentration of the peptide that completely inhibited bacterial growth. Data are representative of three independent experiments

Spectra of Chensinin-1b and its Lipo-Analogs when Interacting with ctDNA

The nature of the interactions between the peptides and ctDNA was monitored via UV spectrometry. As shown in Fig. 2, the concentration of ctDNA was kept constant and the characteristic absorbance peak of ctDNA was detected at 260 nm. Subsequently, peptides were added at increasing concentrations, and the molar ratio of ctDNA:peptide was decreased from 1:0.5 to 1:8. The absorbance intensity of the ctDNA at 260 nm changed significantly. For chensinin-1b, the absorbance at 260 nm increased from OD 0.39 to OD 0.52 as the concentration of the peptide was increased. A similar trend was observed when lipo-chensinin-1b peptides were added. For OA-C1b, the absorbance of ctDNA increased from OD 0.29 to OD 0.38. For LA-C1b, the absorbance increased from OD 0.33 to OD 0.44, and for PA-C1b, the absorbance was increased from OD 0.31 to OD 0.41. The concentration-dependent interaction of the four peptides with ctDNA is shown in Fig. 4a. The binding affinity was reflected in the decrease of OD_{260}, which is the concentration-determining step for this binding reaction. The absorbance at 260 nm for each peptide was modeled using exponential decay functions to obtain the kinetic values (k) of 0.36 (chensinin-1b), 0.67 (OA-C1b), 0.82 (LA-C1b) and 1.99 (PA-C1b); this indicated that the binding affinities of the peptides, in decreasing order, were as follows: PA-C1b > LA-C1b > OA-C1b > chensinin-1b.

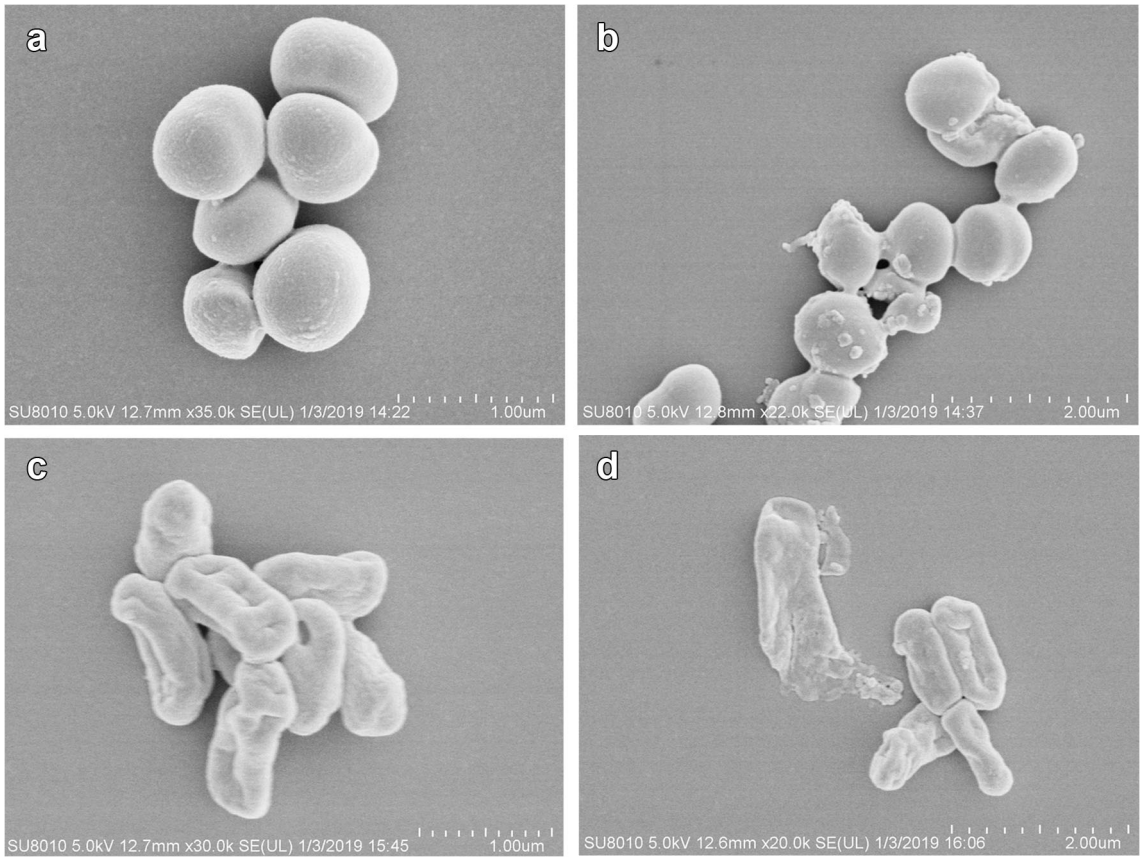

Fig. 1 Scanning electron micrograph of *S. epidermidis* and *E. coli* cells alone (**a**) and (**c**), and in the presence of 1 × the MIC of OA-C1b (**b**) and (**d**). Bacteria (1×10^7 CFU/mL) were incubated with the peptide for 1 h at 37 °C in PBS (pH 7.2), and stained with osmium tetroxide in buffer solution for 2 h, then dehydrated using ethanol

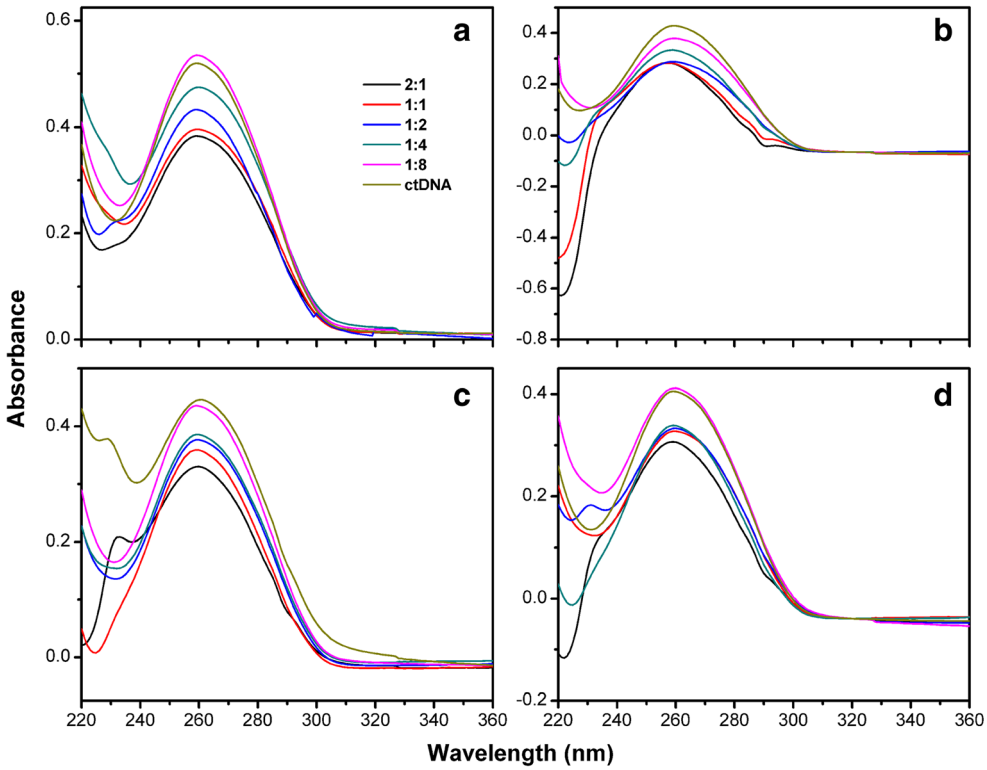

Fig. 2 Molecular interaction of chensinin-1b and its lipo-analogs with ctDNA monitored by UV-Vis spectroscopy: (**a**) chensinin-1b, (**b**) OA-C1b, (**c**) LA-C1b and (**d**) PA-C1b. The spectra of ctDNA in the presence of peptides at increasing concentrations in PBS buffer and were recorded in the range of 220–360 nm, the ratio of peptide and ctDNA was abbreviated as P:D in the figure legend

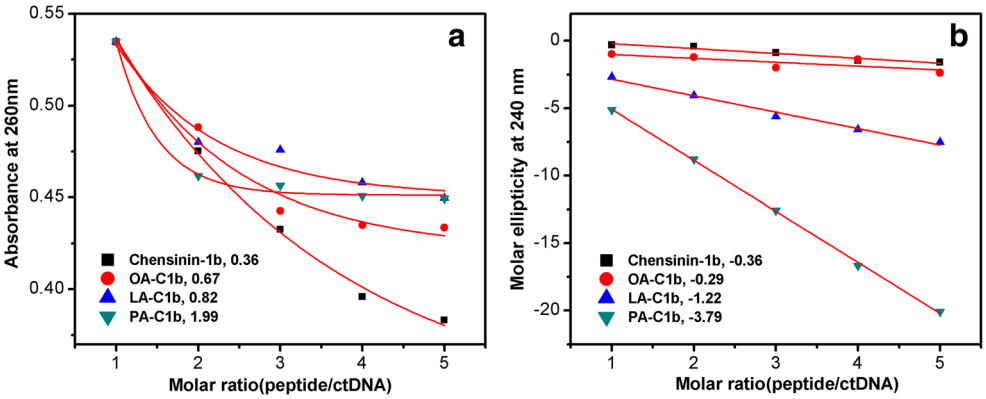

Fig. 4 Concentration dependent courses of the intensity changes in UV-Vis spectra at 260 nm (**a**) and CD spectra at 240 nm (**b**). The decline in the amplitude was modeled by exponential and linear function for UV-vis and CD spectra, respectively. The rate constants are indicated in the legend

Conformational Changes in ctDNA Determined Via CD Spectra

To determine whether the peptides are able to induce DNA conformational changes, circular dichroism spectra were recorded following the addition of peptides at varying concentrations to a fixed concentration of ctDNA. The resulting spectra showed an obvious negative band at 245 nm due to polynucleotide helicity, which is characteristic of DNA in right-handed B form; meanwhile, a positive peak at 275 nm indicated the presence of base stacking in the ctDNA. As shown in Fig. 3, for chensinin-1b, two negative bands at 245 and 260 nm were observed once the peptide was added, and the intensity of the two bands decreased as the molar ratio of peptide:DNA increased from 1 to 5; the obvious peak at 275 nm almost completely disappeared, which indicated that the presence of base stacking was decreased. Comparatively, only one obvious band at 245 nm was observed during incubation with the OA-C1b, LA-C1b and PA-C1b peptides, and the intensity of the band decreased as the peptide concentration increased, which indicated that the degree of helical conformation was increased. The intensity of the peak at 240 nm was plotted as shown in Fig. 4b. The trends showing a decrease were simulated using a linear equation, which showed that the slope (k values) for each peptide was −0.36 (chensinin-1b), −0.29 (OA-C1b), −1.22 (LA-C1b) and −3.79 (PA-C1b), respectively. Based on the slope changes, the ability of the peptides to induce a helical conformation, in

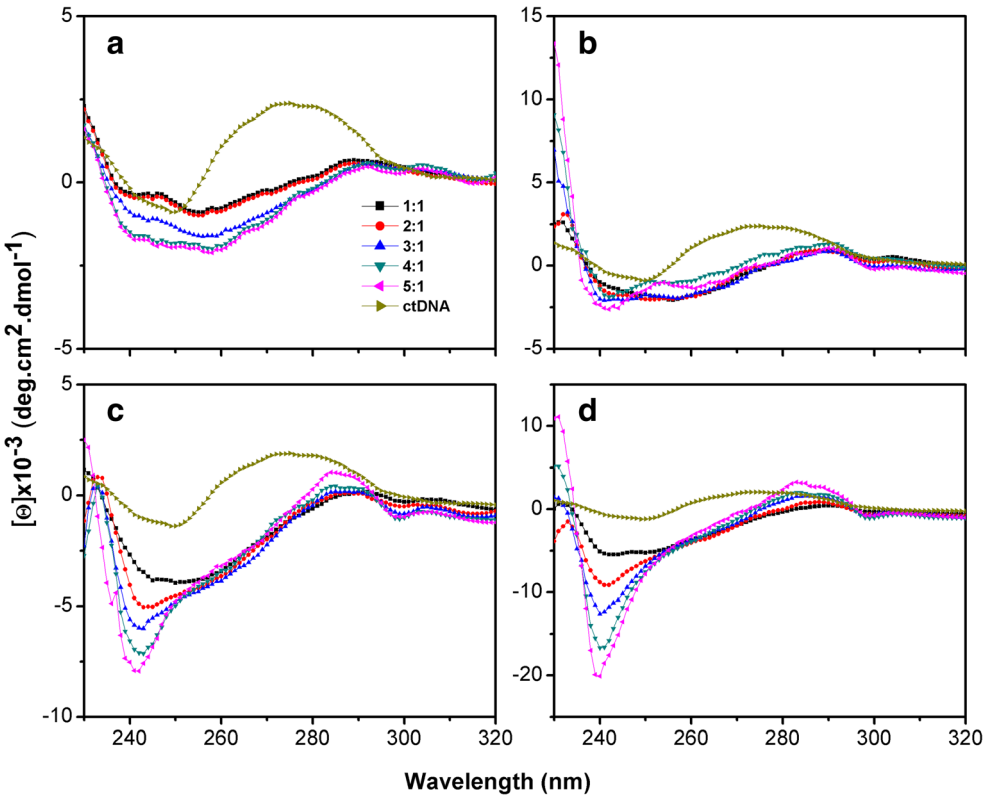

Fig. 3 Molecular interaction of chensinin-1b and its lipo-analogs with ctDNA monitored by CD spectroscopy: (**a**) chensinin-1b, (**b**) OA-C1b, (**c**) LA-C1b and (**d**) PA-C1b. The spectra of ctDNA in the presence of increasing concentration of the peptides in PBS buffer were recorded in the 230–320 nm range, the ratio of peptide and ctDNA was abbreviated as P:D in the figure legend

decreasing order, is as follows: PA-C1b > LA-C1b > OA-C1b ~ chensinin-1b. For LA-C1b and PA-C1b, the bands at approximately 280 nm were slightly more intense when the molar ratio of the peptide: ctDNA was 5:1, indicating that base stacking was increased.

Agarose Gel Electrophoresis

Agarose gel electrophoresis experiments were performed to assess the ability of the peptides to bind to ctDNA. The concentration of ctDNA was fixed while the molar ratio of ctDNA and peptide was varied between 0.25 and 1. The agarose gel electrophoresis experiments were performed for 20 min at 80 V, after which the final gels were illuminated by UV light and photographed. As shown in Fig. S1, a clear band for ctDNA was observed for the blank sample in the second well. As the concentration of the four peptides was increased, the fluorescence intensity of the ctDNA in each lane was gradually diminished, which indicated that ctDNA can bind the peptides to form relatively stable complexes and thereby remain in the wells of the gel. The relative fluorescence intensity was measured using the software that was supplied with the instrument. Based on comparison of the fluorescence intensity of the ctDNA in the second lane, the binding rates were 49.51%, 57.22%, 33.48% and 59.34% for chensinin-1b, OA-C1b, LA-C1b and PA-C1b, respectively, when the molar ratio of ctDNA: peptide was 1:1.

Fluorescence Spectroscopy

Trp fluorescence spectra for chensinin-1b and its lipo-analogs was measured and used to determine the binding affinity of the peptides for ctDNA. As shown in Fig. 5, when chensinin-1b and its lipo-analogs were measured in an aqueous solution, they exhibited a maximum absorption peak at approximately 345 nm, which indicated that the Trp residues in the sequences were completely exposed in the aqueous environment. After ctDNA was added at a molar ratio of chensinin-1b: ctDNA of 0.25, the fluorescence was almost completely quenched by the ctDNA and the maximum absorbance peak occurred at approximately 345 nm; as the ctDNA concentration decreased, the emission fluorescence intensity increased. For OA-C1b, when the molar ratio of OA-C1b and ctDNA was 0.25, a blue-shifted wavelength emission at 336 nm was observed and the fluorescence intensity also increased as the ctDNA concentration decreased. Similar trends were also observed for LA-C1b and PA-C1b. The maximum fluorescence shifts in the presence of ctDNA were approximately 9 nm.

Stern-Volmer quenching constants (K_{sv}) can be used to evaluate the ability of Trp residues in the peptide sequences to bind ctDNA. Trp residues can be quenched by the anion quencher KI when exposed to water. This quenching can be analyzed using the Stern-Volmer equation. As shown in Fig. 6, compared to the slopes obtained from Stern-Volmer plots in the absence of ctDNA, the slopes obtained in the presence of KI quencher and ctDNA exhibited a decrease in the K_{sv}, especially for LA-C1b and PA-C1b, which contain longer alkyl chains(Table 2). The lowest slope obtained for PA-C1b in the presence of I^- was approximate 2.0 M^{-1}, which is approximately 1/4 of that obtained for chensinin-1b. A lower K_{sv} value indicated that the Trp residues were located within a hydrophobic region that could not be accessed by KI, and indicates that the LA-C1b and PA-C1b peptides are able to tightly bind to DNA. When the temperature increased to 37 °C, the slopes exhibited an increase in the K_{sv}, which showed almost no obvious difference.

Evidence of the Formation of ctDNA-Peptide Complexes

The formation of ctDNA-peptide complexes was monitored using DLS experiments. Initially, both ctDNA and the peptides exhibited a single distribution peak and the average diameters size was 8 and 13 nm, respectively (Fig. 7). The most abundant particle distribution was mainly observed at 44 nm when chensinin-1b was added into the DNA solution and allowed to incubate for15-min; for OA-C1b, the most abundant particle sizes was observed to be 164 nm. Similarly, the particle size for LA-C1b was observed to be 32 nm, and 106 nm for PA-C1b. All observations indicated that larger ctDNA-chensinin-1b aggregates were formed.

Viscosity Measurements

Viscosity experiments are useful for determining the mode utilized during the binding of small peptides to ctDNA. Measurements were performed by varying the concentration of peptide that was added to a fixed concentration of ctDNA. The changes in the relative viscosity of ctDNA in the presence of various concentrations of peptides are shown in Fig. 8a. The relative viscosity of ctDNA decreased as the concentration of peptide increased, and the changes in the viscosity slopes, in decreasing order, were as follows: PA-C1b > LA-C1b > OA-C1b > chensinin-1b; this indicated that a nonclassical intercalation mode was utilized using the interaction of antimicrobial peptides with ctDNA.

Zeta Potential Changes in ctDNA in the Presence of the Peptides

Zeta potential measurements were performed to evaluate the charge neutralization ability of the peptides in the presence of

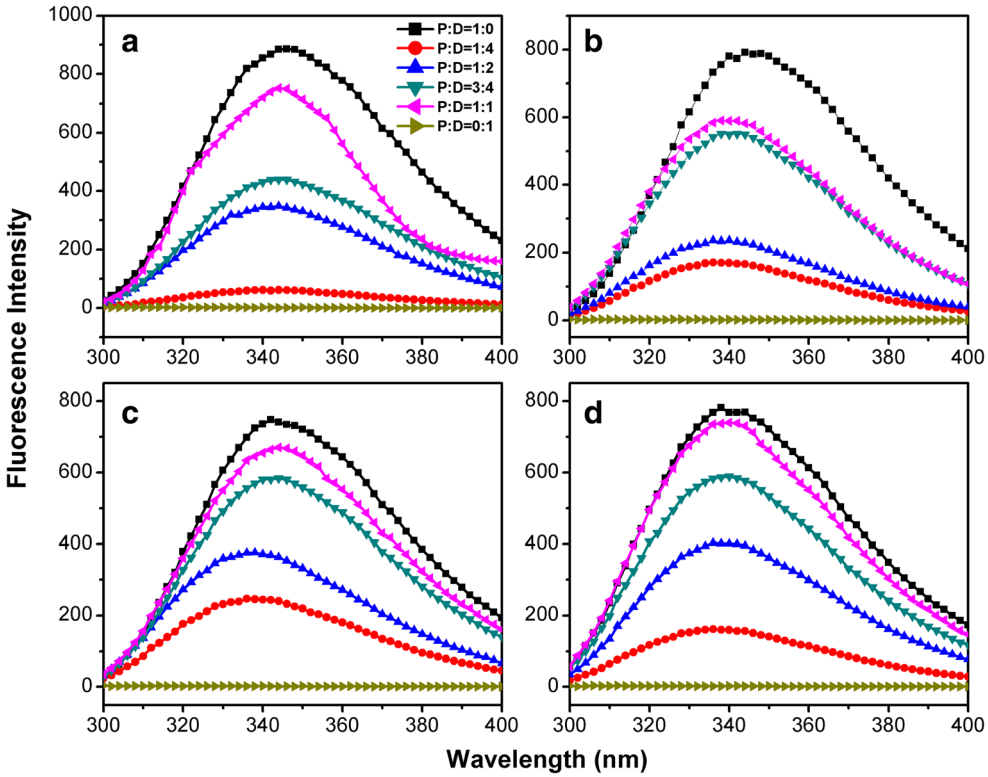

Fig. 5 Trp fluorescence spectra of chensinin-1b and its lipo-analogs with ctDNA at 25 °C. The four peptides were incubated with ctDNA with increasing concentration, (**a**) chensinin-1b, (**b**) OA-C1b, (**c**) LA-C1b and (**d**) PA-C1b

ctDNA. As shown in Fig. 8b, a negative zeta potential of approximately −9.51 mV was observed for ctDNA alone. The addition of increasing concentrations of peptides was able to effectively neutralize the negative charges in the ctDNA. When chensinin-1b was incubated with ctDNA at a final peptide: ctDNA molar ratio of 0.125:1, the zeta potential was increased to −2.37 mV. The zeta potential was increased to −1.27, −1.43 and − 1.07 mV upon addition of the same concentration of OA-C1b, LA-C1b and PA-C1b, respectively. When the peptide: ctDNA molar ratio was increased to 0.25:1, an overcompensation of charges was observed for the four peptides and the resulting zeta potentials were 0.29, 0.13, 1.43 and 2.71 mV for chensinin-1b, OA-C1b, LA-C1b and PA-C1b, respectively, indicating that the pure charge compensation capability of PA-C1b was greater than that of the other three peptides.

Discussion

In the present study, we investigated the antimicrobial activities of lipo-chensinin-1b peptide against selected multidrug-resistant bacterial strains. The parent peptide chensinin-1b, exhibited potent antibacterial activity against several specific multidrug-resistant bacterial strains, including *E. coli* (MREC0203), *S.aureus* (MRSA0910), *E. faecium* (MREF0321) and *S. epidermidis* (MRSE1208), as demonstrated by MIC values that were less than 12.5 μM [26]. Compared with chensinin-1b, the lipo-chensinin-1b peptides exhibited different degrees of antimicrobial activity against bacteria. OA-C1b exhibited potent activity against all tested bacterial strains except *P. aeruginosa* (MRPA0108), *K. pneumonia* (MRKP1112), *E. cloacae* (MREC0320) and *E. aerogenes* (MREA0320), which all

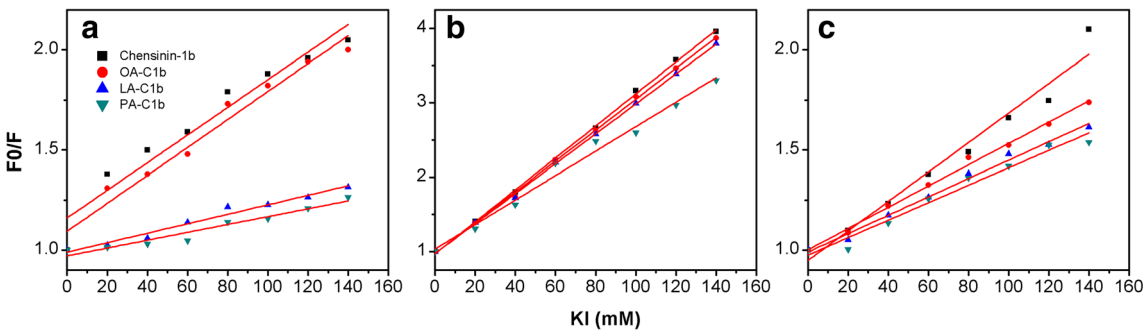

Fig. 6 The Stern-Volmer plots for the fluorescence quenching of Trp residues in the presence of ctDNA at 25 °C (**a**) and 37 °C (**b**) and aqueous buffer (**c**) by KI

Table 2 K_{sv} in PBS buffer or in the presence of ctDNA

Peptide	K_{sv} (M^{-1}) (quenched by KI)		
	Buffer	ctDNA(25 °C)	ctDNA(37 °C)
Chensinin-1b	7.4	6.9	21
OA-C1b	5.3	7.0	21
LA-C1b	4.6	2.4	20
PA-C1b	4.4	2.0	16

had MIC values were greater than 12.5 μM. However, due to the increased length of the aliphatic chains, the antimicrobial activity of LA-C1b was decreased and was almost completely lost in the case of PA-C1b peptide. The results were totally opposite previously published results for cheninin-1, in which the antimicrobial activity of the mutant chensinin-1 peptides was greatly increased due to increased hydrophobicity resulting from the replacement of three Gly residues in the sequence with Trp residues [24]. Multiple linear regression was performed with several functions of 1/MIC as the dependent variable and one, two, or three independent variables-mean hydrophobicity, mean hydrophobic moment, and α-helix content [27]. In our experiments, the attachment of aliphatic acid to the peptide increased the activity against multi-drug resistant bacteria as the length increasing of aliphatic chain, which indicated that 1/MIC is much more affected by hydrophobicity.

AMPs generally serve as one of the primary defense strategies in nature, and they affect cell wall synthesis, transmembrane pore formation, and binding to DNA [28, 29]. DNA plays an important role in the synthesis of proteins, cell proliferation and is the intracellular target of various antibiotics [30]. In the current study, we investigated the interaction of ctDNA with the antimicrobial peptide chensinin-1b and its lipo-analogs. Using UV-vis spectroscopy to observe the interaction of ctDNA with the peptides, a hypochromic effect was observed that was reflected in the exponential decrease in the absorbance intensity, which could be due to base stacking in the ctDNA caused by the interaction of the peptides with hydrophobic environments [31, 32]. In addition, isosbestic points were not observed, which also reflected the binding interaction of ctDNA and the peptides [33].

Both chensinin-1 and its chensinin-1b analog mainly exhibit a random coil conformation in membrane environment according to published CD spectra results [34]. In addition, most chemotherapeutic pharmaceuticals can interact with DNA via several different binding modes, including DNA intercalation, covalent binding, groove binding and electrostatic interaction [35]. However, the conformational changes of DNA when interacting with antimicrobial peptide chensinin-1b have not been fully understood. Therefore, the binding interactions and conformational changes in ctDNA were directly observed using CD spectroscopy. ctDNA exhibited a broad signal during CD spectroscopy, and two negative

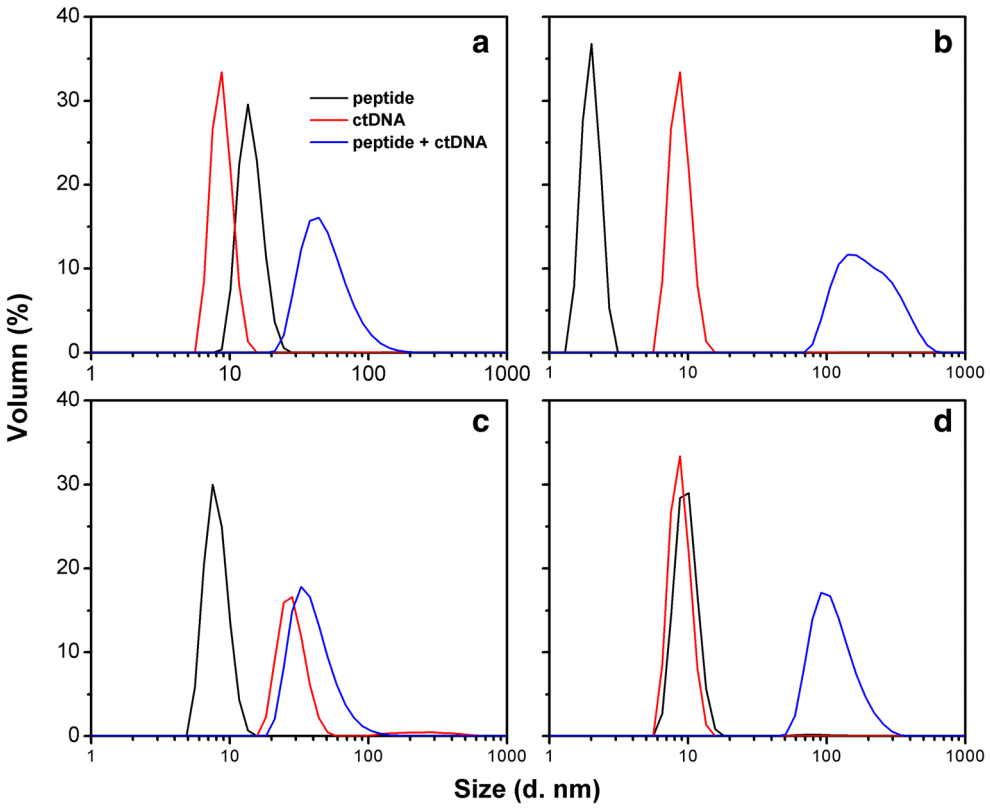

Fig. 7 The formation of ctDNA-peptide complexes monitored by DLS experiments. The peptides were incubated with ctDNA for 15 min (**a**) chensinin-1b, (**b**) OA-C1b, (**c**) LA-C1b and (**d**) PA-C1b

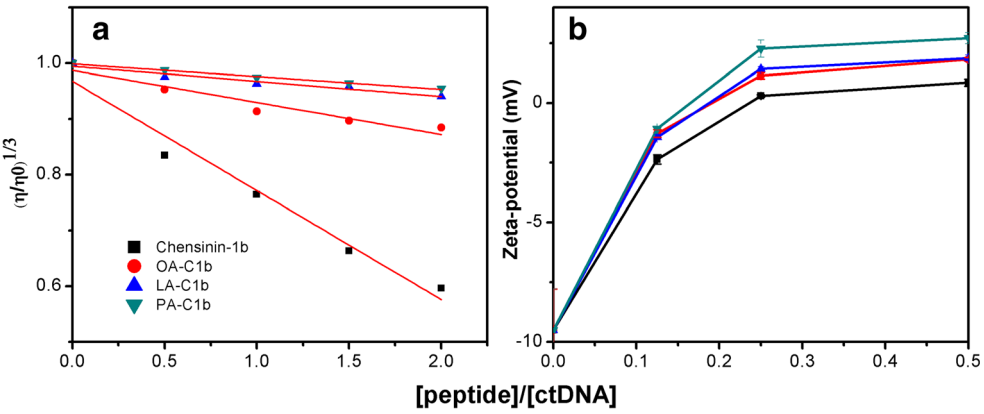

Fig. 8 The relative viscosity of ctDNA affected by the increasing concentration of the peptides (**a**) and the neutralization ability of the cationic peptides on the negative charge of ctDNA (**b**)

peaks were observed at approximately 240 nm and 260 nm during its interaction with chensinin-1b (which didnot contain an aliphatic chain). The presence of the negative band reflected the helicity of the right-handed B form of the ctDNA, and the amount of helicity slightly increased as the concentration of chensinin-1b increased [36]. In the presence of the lipo-chensinin-1b analogs with attached aliphatic chains, the broad band gradually became sharper as the molar ratio of ctDNA and OA-C1b was increased, and the peak at 260 nm was as obvious as the broad band. Similarly, for LA-C1b, an obvious peak at 240 nm was observed that increased in intensity as the concentration of peptide was increased; meanwhile, the peak at approximately 260 nm didnot change in intensity. Furthermore, as the length of the lipophilic alkyl chain was increased, only a single peak at 240 nm was observed, and no peak was observed at 260 nm. These observations indicated that the ctDNA strands were more efficiently wound as the length of the lipophilic alkyl chain increased, which likely arises from the hydrophobicity increase of the peptide and insertion between the DNA bases [37]. The presence of these hydrophobic alkyl chains gives them the additional properties of various modes of aggregation upon dispersal in buffer [20], and the alkyl chains can interact with the hydrophobic interior of the DNA. The propensity of the alkyl chains of the lipo-chensinin-1b peptides to interact with the hydrophobic interior of DNA is further necessitated from the spontaneous tendency of surfactant hydrocarbon chains to minimize water contacts. In addition, the binding interaction of lipo-chensinin-1b peptides with DNA might also lead to important changes in the 'structure' of water molecules around the DNA backbone [38].

To determine the binding mode of the antimicrobial peptides with ctDNA, fluorescence quenching in the absence and presence of ctDNA was measured using potassium iodide as the quencher. ctDNA contains a phosphate anchor that is negatively charged; thus, anionic quenchers are readily repelled by it [39]. Non-intercalative binding plays a vital role in the interaction of the fluorophore, which is located in the outside environment. KI can quench Trp fluorescence both in the presence and absence of ctDNA. Based on this, the K_{sv} values were calculated using the Stern-Volmer equation, and the decrease in K_{sv} values, both in the presence and absence of ctDNA, occurred in the following order: chensinin-1b~OA-C1b > LA-C1b~PA-C1b, which could suggest that the length of the lipophilic alkyl chain and temperature were balanced for K_{sv} values; while when the temperature was set at 37 °C, the data showed a good correlation. These observations were also verified using viscosity measurements. Viscosity was considered to be a convincing method to determine the binding mode utilized by the antimicrobial peptides and ctDNA, as it is sensitive to changes in the length of the ctDNA [40]. While electrostatic interaction may cause the compactness and aggregation of DNA, and the aggregation reduces the number of independently moving DNA molecules which results in lowering of the solution viscosity [41]. Therefore, considering both the electrostatic and hydrophobic interaction, the overall utilization of the classical intercalative mode finally induce a significant increase in the viscosity of the DNA solution, since small molecule intercalative agents could finally separate the base pairs and thus increase the length of the DNA. However, the non-classical groove binding and electrostatic binding interaction modes could cause bending of the DNA helix and reduce the length of the DNA, which was quite similar with the previous observations that chensinin-1b and its analogue can strongly bind with phosphate group of LPS via electrostatic interactions between the seven positive charges in the peptides and the negative charges displayed by LPS in solution, as well as hydrophobic interactions [42]. In such cases, the viscosity of the DNA could be reduced or remain unchanged when it interacted with small molecule agents. In our case, the relative viscosity of the ctDNA exhibited obvious decreases as the concentration of the peptides was increased, indicating that the binding mode of the peptides in the presence of ctDNA was electrostatic due to the cationic nature of the peptides and the negative charges in the ctDNA. The changes in the relative viscosity, in decreasing order, were as follows: chensinin-1b > OA-C1b > LA-C1b > PA-C1b, which reflect the fact that, in addition to

electrostatic interactions, hydrophobic interactions also had a great effect on viscosity due to the increase in the length of the lipophilic alkyl tails. The formation of ctDNA-peptide complexes was also confirmed using agarose gel electrophoresis and DLS experiments. The fluorescence intensity of the ctDNA band in the agarose gel gradually became weaker due to the increase in ctDNA-peptide complex formation; the size of the complex was confirmed using DLS experiments.

Conclusion

In this study, the antimicrobial activity of lipo-chensinin-1b peptides against multidrug-resistant bacterial strains was examined. It was shown that chensinin-1b and its lipo-analogs can bind to ctDNA, and this interaction can be investigated using a combination of various biophysical techniques. UV-Vis absorbance, agarose gel electrophoresis and DLS measurements indicated the presence of complex formation between ctDNA and antimicrobial chensinin-1b and its lipo-analogs. The ctDNA exhibited significant conformational changes upon binding with the antimicrobial peptides due to increases in helicity and the loss of base pair stacking. Iodide can promote quenching of Trp fluorescence in both the presence and absence of DNA; viscosity measurements of ctDNA incubated with the antimicrobial peptides indicated that the peptides interacted with ctDNA via an electrostatic binding mode and were not able to intercalate between the base pairs of ctDNA. However, the possibility that the groove binding mode was utilized and cannot be excluded in this case. In general, our findings provided important information about the interactions of ctDNA with chensinin-1b and its analogs that will be valuable for the rational design of chensinin-1b-based antibiotics with greater specific activity and efficacy.

Acknowledgements This study was supported by the National Natural Science Foundation of China (31872225, 21502083 and 31672289), China Postdoctoral Science Foundation (2016 M601330), LiaoNing Revitalization Talents Program (XLYC1807251) and the funding from Dalian Science and Technology Bureau (2017RQ142).

Compliance with Ethical Standards

Conflict of Interest The authors declare that they have no conflict of interest.

References

1. Walsh C (2000) Molecular mechanisms that confer antibacterial drug resistance. Nature 406:775–781
2. Levy SB (1998) Multidrug resistance–a sign of the times. N Engl J Med 338:1376–1378
3. Lewis K (2013) Platforms for antibiotic discovery. Nat Rev Drug Discov 12:371–387
4. Zasloff M (2002) Antimicrobial peptides of multicellular organisms. Nature 415:389–395
5. Yang L, Harroun TA, Weiss TM, Ding L, Huang HW (2001) Barrel-stave model or toroidal model? A case study on melittin pores. Biophys J81:1475–1485
6. Pouny Y, Rapaport D, Mor A, Nicolas P, Shai Y (1992) Interaction of antimicrobial dermaseptin and its fluorescently labeled analogues with phospholipid membranes. Biochemistry 31: 12416–12423
7. Matsuzaki K, Murase O, Fujii N, Miyajima K (1996) An antimicrobial peptide, magainin 2, induced rapid flip-flop of phospholipids coupled with pore formation and peptide translocation. Biochemistry 35:11361–11368
8. Ding L, Yang L, Weiss TM, Waring AJ, Lehrer RI, Huang HW (2003) Interaction of antimicrobial peptides with lipopolysaccharides. Biochemistry 42:12251–12259
9. Li Y, Qi X, Zhang Q, Huang Y, Su Z (2012) Overview on the recent study of antimicrobial peptides: origins, functions, relative mechanisms and application. Peptides 37:207–215
10. Sun Y, Dong W, Sun L, Ma L, Shang D (2015) Insights into the membrane interaction mechanism and antibacterial properties of chensinin-1b. Biomaterials 37:299–311
11. Park CB, Kim HS, Kim SC (1998) Mechanism of action of the antimicrobial peptide buforin II: buforin II kills microorganisms by penetrating the cell membrane and inhibiting cellular functions. Biochem Biophys Res Commun 244:253–257
12. Boman HG, Agerberth B, Boman A (1993) Mechanisms of action on Escherichia coli of cecropin P1 and PR-39, two antibacterial peptides from pig intestine. Infect Immun 61:2978–2984
13. Gupta RC, Spencer-Beach G (1996) Natural and endogenous DNA adducts as detected by 32P-postlabeling. Regul Toxicol Pharmacol 23:14–21
14. Tennant AH, Peng B, Kligerman AD (2001) Genotoxicity studies of three triazine herbicides: in vivo studies using the alkaline single cell gel (SCG) assay. Mutat Res 493:1–10
15. Boer DR, Canals A, Coll M (2009) DNA-binding drugs caught in action: the latest 3D pictures of drug-DNA complexes. Dalton Trans:399–414
16. Pindur U, Jansen M, Lemster T (2005) Advances in DNA-ligands with groove binding, intercalating and/or alkylating activity: chemistry, DNA-binding and biology. Curr Med Chem 12:2805–2847
17. Upadhyay SK (2017) Binding and thermodynamics of REV peptide-ctDNA interaction. Biopolymers 108:e22902
18. Mukherjee A, Mondal S, Singh B (2017) Spectroscopic, electrochemical and molecular docking study of the binding interaction of a small molecule 5H-naptho[2,1-f][1,2] oxathieaphine 2,2-dioxide with calf thymus DNA. Int J Biol Macromol 101:527–535
19. Zhang G, Zhang Y, Zhang Y, Li Y (2013) Spectroscopic studies of cyanazine binding to calf thymus DNA with the use of ethidium bromide as a probe. Sensor Actuat B-Chem 182:453–460
20. Dong W, Liu Z, Sun L, Wang C, Guan Y, Mao X, Shang D (2018) Antimicrobial activity and self-assembly behavior of antimicrobial peptide chensinin-1b with lipophilic alkyl tails. Eur J Med Chem 150:546–558
21. Pal T, Abraham B, Sonnevend A, Jumaa P, Conlon JM (2006) Brevinin-1BYa: a naturally occurring peptide from frog skin with broad-spectrum antibacterial and antifungal properties. Int J Antimicrob Agents 27:525–529
22. Park NG, Lee S, Oishi O, Aoyagi H, Iwanaga S, Yamashita S, Ohno M (1992) Conformation of tachyplesin I from tachypleus tridentatus when interacting with lipid matrices. Biochemistry 31: 12241–12247
23. Beckloff N, Laube D, Castro T, Furgang D, Park S, Perlin D, Clements D, Tang H, Scott RW, Tew GN, Diamond G (2007) Activity of an antimicrobial peptide mimetic against planktonic

and biofilm cultures of oral pathogens. Antimicrob Agents Chemother 51:4125–4132
24. Dong W, Mao X, Guan Y, Kang Y, Shang D (2017) Antimicrobial and anti-inflammatory activities of three chensinin-1 peptides containing mutation of glycine and histidine residues. Sci Rep 7:40228
25. van der Wal A, Minor M, Norde W, Zehnder AJB, Lyklema J (1997) Electrokinetic potential of bacterial cells. Langmuir 13: 165–171
26. Shang D, Meng X, Zhang D, Kou Z (2017) Antibacterial activity of chensinin-1b, a peptide with a random coil conformation, against multiple-drug-resistant Pseudomonas aeruginosa. Biochem Pharmacol 143:65–78
27. Pathak N, Salas-Auvert R, Ruche G, Janna MH, McCarthy D, Harrison RG (1995) Comparison of the effects of hydrophobicity, amphiphilicity, and alpha-helicity on the activities of antimicrobial peptides. Proteins. 22:182–186
28. Brogden KA (2005) Antimicrobial peptides: pore formers or metabolic inhibitors in bacteria? Nat Rev Microbiol 3:238–250
29. Kawasaki H, Koyama T, Conlon JM, Yamakura F, Iwamuro S (2008) Antimicrobial action of histone H_2B in Escherichia coli: evidence for membrane translocation and DNA-binding of a histone H_2B fragment after proteolytic cleavage by outer membrane proteinase T. Biochimie 90:1693–1702
30. Subastri A, Ramamurthy CH, Suyavaran A, Mareeswaran R, Lokeswara Rao P, Harikrishna M, Suresh Kumar M, Sujatha V, Thirunavukkarasu C (2015) Spectroscopic and molecular docking studies on the interaction of troxerutin with DNA. Int J Biol Macromol 78:122–129
31. Shahabadi N, Maghsudi M (2014) Multi-spectroscopic and molecular modeling studies on the interaction of antihypertensive drug; methyldopa with calf thymus DNA. Mol BioSyst 10:338–347
32. Fu XB, Liu DD, Lin Y, Hu W, Mao ZW, Le XY (2014) Water-soluble DNA minor groove binders as potential chemotherapeutic agents: synthesis, characterization, DNA binding and cleavage, antioxidation, cytotoxicity and HSA interactions. Dalton Trans: 8721–8737
33. Sirajuddin M, Ali S, Badshah A (2013) Drug–DNA interactions and their study by UV–visible, fluorescence spectroscopies and cyclic voltametry. J Photochem Photobiol B 124:1–19
34. Dong W, Sun Y, Shang D (2015) Interactions between chensinin-1, a natural antimicrobial peptide derived from Rana chensinensis, and lipopolysaccharide. Biopolymers 103:719–726
35. Erkkila KE, Odom DT, Barton JK (1999) Recognition and reaction of metallointercalators with DNA. Chem Rev 99:2777–2799
36. Mati SS, Roy SS, Chall S, Bhattacharya S, Bhattacharya SC (2013) Unveiling the groove binding mechanism of a biocompatible naphthalimide-based organoselenocyanate with calf thymus DNA: an "ex vivo" fluorescence imaging application appended by biophysical experiments and molecular docking simulations. J Phys Chem B 117:14655–14665
37. Ranjbar B, Gill P (2009) Circular dichroism techniques: biomolecular and nanostructural analyses- a review. Chem Biol Drug Des 74: 101–120
38. Bhattacharya S, Mandal SS (1997) Interaction of surfactants with DNA. Role of hydrophobicity and surface charge on intercalation and DNA melting. Biochim Biophys Acta 1323:29–44
39. Zhou X, Zhang G, Wang L (2014) Probing the binding mode of psoralen to calf thymus DNA. Int J Biol Macromol 67:228–237
40. Macías B, Villa MV, Lapresa R, Alzuet G, Hernández-Gil J, Sanz F (2012) Mn(II) complexes with sulfonamides as ligands. DNA interaction studies and nuclease activity. J Inorg Biochem 115:64–71
41. Shah A, Zaheer M, Qureshi R, Akhter Z, Nazar MF (2010) Voltammetric and spectroscopic investigations of 4-nitrophenylferrocene interacting with DNA. Spectrochim Acta A Mol Biomol Spectrosc 75:1082–1087
42. Dong W, Dong Z, Mao X, Sun Y, Li F, Shang D (2016) Structure-activity analysis and biological studies of chensinin-1b analogues. Acta Biomater 37:59–68